NASA Technical Memorandum 78708

HIGH FREQUENCY SOUND ATTENUATION IN SHORT FLOW DUCTS

(NASA-TM-78708) HIGH FREQUENCY SOUND ATTENUATION IN SHORT FLOW DUCTS (NASA) 25 p HC A02/MF A01 CSCL 20A

N78-23876

Unclas

G3/71 16770

J. W. Posey

May 1978

NASA
National Aeronautics and Space Administration
Langley Research Center
Hampton, Virginia 23665

SUMMARY

A geometrical acoustics approach is proposed as a practical design tool for absorbent liners in such short flow ducts as may be found in turbofan engine nacelles. As an example, a detailed methodology is presented for three different types of sources in a parallel plate duct containing uniform ambient flow. A plane wave whose wavefronts are not normal to the duct walls, an arbitrarily located point source, and a spatially harmonic line source are each considered. Optimal wall admittance distributions are found, and it is shown how to estimate the insertion loss for any admittance distribution. It is suggested that the extension of the methodology to realistic source distributions in variable area cylindrical or annular ducts containing arbitrary flow is conceptually straightforward and computationally practical on a vector-hardware digital computer.

INTRODUCTION

The study of sound transmission and attenuation in soft walled flow ducts has received considerable attention since the advent of jet-powered commercial transport aircraft in the late 1950's (see refs. 1 and 2 for reviews of this work). The foundation for much of this work was laid earlier by Cremer (ref. 3), who investigated the infinite uniform duct problem. Cremer concluded that regardless of the original pressure distribution of an acoustical disturbance, there will be a finite distance down the duct past which the lowest order, or least attenuated, mode will dominate the sound field. He suggested that overall sound attenuation would be maximized by maximizing the attenuation of the least attenuated mode. An excellent exposition and extension of Cremer's work is given by Tester in reference 4.

Tyler and Sofrin (ref. 5) were the first to emphasize the importance of the higher order duct modes in the turbomachinery noise problem, and Zorumski (ref. 6) presented a systematic analytical approach to account for modal propagation (transmission and reflection) in finite ducts having multi-segment liners. Rice (ref. 7) has developed a liner design technique based on an observed collapse of infinite-duct modal characteristics with cutoff ratio, and Nayfeh, et al., (ref. 8) have derived a modal propagation algorithm for variable area ducts.

As modal theory has been applied to more complex duct and flow configurations, physical interpretations have become imprecise and computational problems (eigenvalue calculations most notably) have become more formidable. In attempts to circumvent some of the problems inherent in modal calculations, a number of numerical field solution algorithms have been developed (refs. 9, 10, and 11). Such numerical procedures are powerful tools for attacking problems involving arbitrary duct shapes, arbitrary flows, complicated source distributions and variable boundary conditions. However, numerics go directly from governing equations to resultant pressure distributions, providing no direct physical insight into mechanisms of propagation, reflection and attenuation.

Geometrical acoustics avoids many of the modal calculation proglems, and it also provides the physical insight lacking in purely numerical approaches. Ray theory has been employed by Wright (ref. 12) to compare noise radiation from free field and ducted rotors, by Tester (ref. 13) to develop some insight into why modal attenuation is maximized in an infinite duct by use of the Cremer optimal impedance, and by Lester and Posey (ref. 13) to verify the optimal wall impedance and maximum attenuation calculated from modal theory for a point source in a finite cylindrical duct. These studies indicate that geometrical theories can be used with confidence in short ducts and when wavelengths are much less than the duct height or diameter, as is often the case in turbofan inlets and short exhaust ducts. As an example application, the present paper utilizes geometrical acoustics to develop design procedures for absorptive liners in short parallel plate flow ducts for three types of high frequency acoustical sources: a plane wave with arbitrary angle of incidence on the walls, a point source and a line source. For each source type it is shown how to determine the wall admittance distribution which maximizes sound absorption and how to estimate the insertion loss for an arbitrary admittance distribution.

PARALLEL PLATE DUCT

The coordinate system for the parallel plate geometry is shown in figure 1. The two semi-infinite plates occupy the planes $y = \pm h$ for $z \leq d$. There is a uniform flow in the z direction of Mach number M.

Plane wave propagation.- First, consider the idealized case where the sound field at $z = 0$ can be represented as a plane wave with wavefronts normal to the y-z plane and making an angle θ with the z-axis. Then the unit vector $\vec{n}$ normal to the wavefronts makes an angle θ with the vertical. In the absence of flow, Huygen's Principle states that the wavefronts advance at the speed of sound c. In a uniform flow, the wavefronts still advance with the speed of sound in a reference frame moving with the medium, but the field is also convected with the medium at a velocity $cM\vec{e}_z$ where $\vec{e}_z$ is a unit vector in the z direction. Thus, the rays are no longer normal to the wavefronts, but rather propagate in the direction of the vector $\vec{n} + M\vec{e}_z$ as shown in figure 2. The angle of incidence of the rays on the wall (the angle that the ray makes with vertical) is given by θ_R where

$$\tan \theta_R = \frac{M + \sin \theta}{\cos \theta} \tag{1}$$

It is clear that only waves with θ_R in the range $(0, \pi)$ carry energy toward the duct termination. Due to symmetry about $\theta_R = \pi/2$, attention is further limited in this section to θ_R in $(0, \pi/2)$ with no loss in generality. Therefore, $\tan \theta_R \geq 0$ or $\sin \theta \geq -M$. If $M < 0$, then flow is coming into the duct and convection will prevent the escape of any acoustical energy unless the z component of $\vec{n}$ exceeds $|M|$.

Tester (ref. 13) has considered this problem in some detail where the incident plane wave pressure field is given by $p_i \exp(ik_y y + ik_z z - i\omega t)$ and the reflected wave by $p_r \exp(-ik_y y + ik_z z - i\omega t)$. Requiring continuity of particle displacement between the wall and the fluid and defining the specific normal admittance in the usual manner, $\beta \equiv \rho_o c \left(\frac{u_y}{p}\right)_{wall}$, Tester obtains a pressure reflection coefficient $C_r \equiv p_r/p_i$ given by

$$C_r = \frac{\cos\theta - \beta(1 - M\sin\theta)^2}{\cos\theta + \beta(1 - M\sin\theta)^2} \qquad (2)$$

Notice that complete absorption occurs when the admittance is

$$\beta_{opt} = (1 - M\sin\theta)^{-2}\cos\theta \qquad (3)$$

That is, the optimal duct liner has zero reactance and a specific resistance R_{opt} equal to β_{opt}^{-1}.

$$R_{opt} = (1 - M\sin\theta)^2/\cos\theta \qquad (4)$$

Optimal resistance as a function of wavefront orientation is plotted in figure 3 for both inflow and exhaust. The Mach number magnitude is arbitrarily set to 0.35. These curves suggest that designing a liner for the attenuation of random incidence noise may be more easily accomplished in an exhaust duct than in an inlet duct due to the relative flatness of the curve for the exhaust case. That is, a normal specific resistance of unity would be near optimal for a wide range of wavefront orientations ($-20° < \theta < 70°$ in the present case) for propagation with the flow, while no resistance value would yield similar performance for propagation against the flow.

For a specific design problem where a range of θ or θ_R is specified along with a range of Mach numbers, equations 1 and 4 can be used to construct a family of curves similar to those in figure 3 from which a target value for the resistance can be chosen. An estimate of the transmission loss for any given M, θ, duct height 2h and distance to duct termination d is readily obtained by adding the fraction of the incident power which is radiated directly to the fraction which is radiated after a single reflection, as illustrated in figure 4. Let F_D be the fraction of the rays which radiate without reflection and F_r the fraction which are reflected. The power reflection coefficient is $|C_r|^2$, so that the insertion loss is approximately

$$IL \cong -10 \log(F_D + F_r|C_r|^2) \tag{5}$$

Multiple reflections can be similarly taken into account.

A better estimate of the transmission loss could be found by employing ray scattering theory as presented by Felsen and Yee (ref. 15).

<u>Point source</u>.- When a point source is radiating into a stationary medium, the resulting wavefronts are concentric spheres, as shown in figure 5a. If the source remains stationary, but the medium has a uniform flow Mach number M, then the wavefronts are still spherical, but they are no longer concentric, since they are convected downstream as they expand (see figure 5b). However, the ray paths are straight in either case (ref. 16). Thus, for a point source at $(0, h_s, 0)$ in the parallel plate duct of figure 1, the angle of incidence for direct rays on the duct wall at $(x, \pm h, z)$ is given by

$$\theta_R = \arctan \frac{(x^2 + z^2)^{\frac{1}{2}}}{\pm h - h_s}$$

The wavefronts may be considered locally plane when $k\ x^2 + z^2 + (h \pm h_s)^2\ ^{\frac{1}{2}} >> 1$, and an analysis along the lines of that used by Tester (ref. 13) in deriving equation 2 yields the following expression for the complex pressure reflection factor.

$$C_r \cong \frac{\cos\theta_y - \beta(1 - M\cos\theta_z)^2}{\cos\theta_y + \beta(1 - M\cos\theta_z)^2} \tag{7}$$

Here, θ_y is the angle which the wavefront normal makes with the $\vec{e}_y$ vector and θ_z is the angle it makes with $\vec{e}_z$. Equation 7 could be adjusted to account for the curvature of the wavefronts (see ref. 17), but this is beyond the scope of this paper.

In order for equation 7 to be utilized in determining an optimal impedance distribution $\beta_{opt}(x, \pm h, z)$, the wavefront orientation angles θ_y and θ_z must be expressed as functions of position on the walls. It is convenient to define ϕ as the angle which the ray makes with $\vec{e}_z$. That is,

$$\phi = \arctan \frac{\left[(\pm h - h_s)^2 + x^2\right]^{1/2}}{z} \tag{8}$$

Since the ray propagates in a straight line with the velocity $c\vec{n} + cM\vec{e}_z$, it can be shown that

$$\tan\phi = \frac{\sin\theta_z}{M + \cos\theta_z} \tag{9}$$

Equations 8 and 9 combine to give

$$\frac{\sin\theta_z}{M + \cos\theta_z} = \left[(\pm h - h_s)^2 + x^2\right]^{1/2} z^{-1} \tag{10}$$

Since the flow is parallel to $\vec{e}_z$, the center of curvature of any wavefront will always lie on the line $y = h_s$, $x = 0$. Thus, once θ_z is determined from equation 10, θ_y can be found from

$$\cos \theta_y = \frac{\pm \sin \theta_z}{\left[1 + x^2/(\pm h - h_s)^2\right]^{\frac{1}{2}}} \tag{11}$$

Now that the wavefront orientation angles θ_y and θ_z can be determined for any wall position by using equations 10 and 11, equation 7 can be used to determine the reflection coefficient at any wall position for an arbitrary admittance β at that point. As with a plane wave source, C_r can be nulled. In the present case, this is accomplished by

$$\beta_{opt}(x, \pm h, z, M) = \frac{\cos \theta_y(x, \pm h, z)}{[1 - M \cos \theta_z(x, \pm h, z)]^2} \ . \tag{12}$$

Again, β_{opt} is real, implying that the optimal reactance is zero and that the optimal resistance R_{opt} is given by β_{opt}^{-1}, which is now position dependent.

If it is not possible to vary the wall admittance continuously, as dictated by equation 12, then the designer could divide the liner into uniform segments such that β_{opt} had little variation over any one of the segments. In determining the average value of β_{opt} over a segment, the appropriate weighting function is the density of direct rays incident on the wall as a function of position (proportional to energy flux per unit area, not to be confused with wave intensity). The ray density over one of the spherical wavefronts is inversely proportional to the square of the radius of curvature of that wavefront, but the surface of maximum density is locally normal to the direction of ray propagation. Let $\vec{e}_r(x, y, z)$ be a unit vector in the direction of the ray path, then the local density of rays through the surface normal to $\vec{e}_r$ is proportional to $\left[r_c^2(\vec{n} \cdot \vec{e}_r)\right]^{-1}$. It follows that the density of rays incident on the wall is

$$D(x, \pm h, z) = A \frac{\cos \theta_R}{r_c^2(\vec{n} \cdot \vec{e}_r)} , \qquad (13)$$

where A is the constant of proportionality and r_c is the radius of curvature of the wavefront, given by

$$r_c = \frac{\left[x^2 + (y - h_s)^2\right]^{1/2}}{\sin \theta_z} \qquad (14)$$

Once a distribution of β has been selected by the designer, the resulting insertion loss can be estimated by approximating P_L, the power radiated from the lined duct, as the sum of the direct radiation and that carried by rays which escape the duct after one and only one reflection. Such singly reflected rays strike the walls at $z > z^{\pm}$ where

$$z^{\pm} = \frac{(h \mp h_s)d}{2h + h_s} , \quad y = \pm h \qquad (15)$$

Thus,

$$P_L \cong \int_{z^+}^{d} \int_{-\infty}^{\infty} D(x, h, z) |C_r(x, h, z)|^2 dxdz + \int_{z^-}^{d} \int_{-\infty}^{\infty} D(x, -h, z) |C_r(x, -h, z)|^2 dxdz$$

$$+ \int_{-h}^{h} \int_{-\infty}^{\infty} \frac{Ad}{r_c^2(\vec{n} \cdot \vec{e}_r)} \left[d^2 + x^2 + (y - h_s)^2\right]^{-1/2} dxdy \qquad (16)$$

where C_r is the pressure reflection coefficient given by equation 7. The inclusion of multiply-reflected rays is straightforward, but beyond the scope of this paper. The radiated power from the corresponding hardwalled duct is

$$P_H = \int_0^d \int_{-\infty}^{\infty} \left[D(x, h, z) + D(x, -h, z)\right] dxdz + \int_{-h}^{h} \int_{-\infty}^{\infty} \frac{Ad}{r_c^2(\vec{n} \cdot \vec{e}_r)} \left[d^2 + x^2 + (y - h_s)^2\right]^{-\frac{1}{2}} dxdy \tag{17}$$

and the insertion loss is

$$IL = -10 \log \frac{P_L}{P_H} \tag{18}$$

Line source.- A line source is taken to lie parallel to $\vec{e}_x$ at $z = 0$, $y = h_s$. The source flux varies as $e^{i(k_s x - \omega t)}$. Hence, in the absence of flow, the wavefronts are right circular cones and have a semi-apex angle given by arccos (k_s/k), where $k = \omega/c$, and c is the ambient speed of sound. The ray density at any point on the wavefront is inversely proportional to the radius of the cross section of the cone, and the rays are normal to the wavefronts. Again imposing the uniform flow velocity $cM\vec{e}_z$, the wavefronts remain right circular cones, but the axes are no longer coincident with the source line. The intersection of a typical wavefront cone with the plane $y = h_s$ is shown in figure 6. Huygen's Principle implies that the position of such a wavefront at any given time may be determined as the envelope of the spherical wavefronts (representing equal phase) from all the points on the source line which the wavefront has passed. Since these spheres are convected at the velocity $cM\vec{e}_z$ as their radii increase at the rate c, and the apex of the conical wavefront advances at a speed of ω/k_s along the line source, it follows that the axis of the conical wavefront lies in the plane $y = h_s$ and makes an angle τ with $\vec{e}_x$.

$$\tan \tau = Mk_s/k \tag{19}$$

Also, the semi-apex angle of the cone is γ, where

$$\tan \gamma = \frac{k_s}{k}\left[1 - \frac{k_s^2}{k^2}(1 - M^2)\right]^{-\frac{1}{2}} \tag{20}$$

Therefore, for $k_s \neq 0$ the instantaneous locations of the wavefronts are given mathematically by the family of surfaces satisfying the following equation.

$$(y - h_s)^2 + [(a - x)\sin\tau + z\cos\tau]^2$$

$$= [(a - x)\cos\tau - z\sin\tau]^2 \tan^2\gamma,\ x \leq a \tag{21}$$

Here, $(a, h_s, 0)$ is the location of the apex of the cone. From equation 21 it is straightforward to determine the relative transverse position of the apex $(a - x)$ for wavefronts which are incident upon the walls $y = \pm h$ at any given axial station z. In particular, $(a - x)$ is the positive root of the quadratic equation

$$C_2(a - x)^2 + C_1(a - x) + C_o = 0 \tag{22}$$

where

$$C_2 = \tan^2 \tau - \tan^2\gamma$$

$$C_1 = 2z \tan \tau(1 + \tan^2\gamma)$$

$$C_c = \frac{(\pm h - h_s)^2}{\cos^2\tau} + z^2(1 - \tan^2\tau \tan^2\gamma)$$

Let ℓ be the length of the line between the point of incidence and the apex of the wavefront. Then from figure 6, it follows that

$$\ell = \left[(a - x)^2 + (\pm h - h_s)^2 + z^2\right]^{1/2} , \tag{23}$$

and $c\Delta t = \ell \tan \gamma$. Thus, the wavefront normal is in the direction of the vector from $[x - \ell \tan \gamma \sin(\tau + \gamma), h_s, M \ell\tan \gamma]$ to $(x, \pm h, z)$.

$$\vec{n} = \frac{\vec{N}}{|\vec{N}|} \tag{24}$$

where

$$\vec{N} = \vec{e}_x \, \ell \tan \gamma \sin(\tau + \gamma) + \vec{e}_y(\pm h - h_s)$$
$$+ \vec{e}_z[z - M \ell \tan \gamma] .$$

Since the components of any unit vector are its direction cosines,

$$\cos \theta_y = \vec{n} \cdot \vec{e}_y$$

and

$$\cos \theta_z = \vec{n} \cdot \vec{e}_z \tag{25}$$

These cosine values can be substituted into equation 7, and nulling the numerator would yield an optimal axial variation of admittance for each wall

$$\beta_{opt}\left(\pm h,\ z,\ M,\ \frac{k_s}{k}\right) = (\pm h - h_s)[1 - M(z - M\ell \tan \gamma)]^{-1} \quad (26)$$

Notice that equation 26 differs from equation 12, the optimal admittance for a point source, in that there is no x dependence, but there is a dependence upon the ratio of the source wave number k_s to the free space wave number $k = \frac{\omega}{c}$. Hence, it would be easier to construct the optimal liner for the line source since it would need to vary in only one direction, but additional information about the source (the values of ω and k_s) would be required.

The ray density on the wavefront is inversely proportional to the radius of spreading, denoted by $c\Delta t$ in figure 6, and equal to $\ell \tan \Upsilon$. As with the point source, the local ray direction must be determined in order to arrive at an expression for the density D_L of direct rays incident on the wall. Specifically, $\vec{e}_r$ is the unit vector in the direction of $\vec{n} + M\vec{e}_z$, and

$$D_L(\pm h,\ z) = \frac{B}{\ell(\pm h,\ z)\tan \Upsilon} \frac{\vec{e}_r \cdot \vec{e}_y}{\vec{n} \cdot \vec{e}_r} \ . \quad (27)$$

Here, B is the constant of proportionality. Thus, if multiply-reflected rays are again neglected, the power radiated per unit length of the source from an off-optimal lined duct is

$$P_L' = \int_{z^+}^{d} D_L(h,\ z)|C_r(h,\ z)|^2\,dz + \int_{z^-}^{d} D_L(-h,\ z)|C_r(-h,\ z)|^2\,dz$$

$$+ \int_{-h}^{h} B[\ell(y,\ d)\tan \gamma]^{-1}\,dy \quad (28)$$

and the power radiated per unit length from a hard walled duct is

$$P_H' = \int_{o}^{d} [D(h, z) + D(-h, z)]dz + \int_{-h}^{h} \mathcal{B}[\ell(y, d)\tan \gamma]^{-1}\, dy \qquad (29)$$

The insertion loss is

$$IL = -10 \log \frac{P_L'}{P_H'} \ . \qquad (30)$$

CONCLUDING REMARKS

In aircraft turbofan engines, the noise that propagates through the inlet and fan exhaust ducts is due to several different mechanisms. Some of these mechanisms, such as the rotor interaction with small scale turbulence, or with a small scale inflow distortion, may be considered as point sources, while others, such as the rotor-locked pressure field, may be considered as a ring source or a series of ring sources. The liner design methodology developed above for point and line sources in a parallel plate duct can be straightforwardly extended in principle to point and ring sources in ducts of arbitrary shape and even to a random distribution of sources within such ducts. Nonlinear liner interactions, the effects of multiple reflections and scattering at duct discontinuities could also be included, and radiation patterns as well as insertion losses could be predicted. Although the implementation of the methodology would involve extensive computer programming, the effects of basic acoustical phenomena such as refraction, diffraction, reflection and absorption could be easily followed through the calculations, a definite advantage over modal or purely numerical approaches.

Ray tracing solutions to such complicated problems as turbomachinery duct noise propagation have been avoided in the past possibly because of prohibitively large computation times being required; however, the recent advent of vector-hardware digital computers makes possible reductions in computation time for such problems of at least an order of magnitude. Therefore, it seems quite within reason that the principles of geometrical acoustics utilized in the example problem of this paper could be the basis of a practical design procedure which employs more realistic source, duct and flow models than are currently used in procedures based on modal theory.

REFERENCES

1. Nayfeh, A. H.; Kaiser, J. E.; and Telionis, D. P.: The Acoustics of Aircraft Engine-Duct Systems. AIAA Journal, vol. 13, February 1975, pp. 130-153.

2. Vaidya, P. G.; and Dean, P. D.: State of the Art in Duct Acoustics. AIAA Paper 77-1279, October 1977.

3. Cremer, L.: Theorie der Luftschall-Dämpfung im Rechteckkanal mit schluckender Wand und das sich dabei ergebende höchste Dämpfungsmass. Acoustica, vol. 3, no. 2, 1953, pp. 249-263.

4. Tester, B. J.: The Optimization of Modal Sound Attenuation in Ducts in the Absence of Mean Flow. J. of Sound and Vibration, vol. 27, no. 4, 1973, pp. 477-513.

5. Tyler, J. M.; and Sofrin, T. G.: Axial Flow Compressor Noise Studies. SAE Transactions, vol. 70, 1962, pp. 309-332.

6. Zorumski, W. E.: Acoustic Theory of Axisymmetric Multisectioned Ducts. NASA TR R-419, 1974.

7. Rice, E. J.: Inlet Noise Suppressor Design Method Based upon the Distribution of Acoustic Power with Mode Cutoff Ratio. NASA CP-2001, vol. 3, 1976, pp. 883.

8. Nayfeh, A. H.; Shaker, B. S.; and Kaiser, J. E.: Transmission of Sound Through Nonuniform Circular Ducts with Compressible Mean Flows. NASA CR-145126, May 1977.

9. Quinn, D. W.: A Finite Difference Method for Computing Sound Propagation in Nonuniform Ducts. AIAA Paper 75-130, January 1975.

10. Baumeister, K. J.: Finite-Difference Theory for Sound Propagation in a Lined Duct with Uniform Flow Using the Wave Envelope Concept. NASA Technical Paper 1001, August 1977.

11. Abrahamson, A. L.: A Finite Element Algorithm for Sound Propagation in Axisymmetric Ducts Containing Compressible Mean Flow. AIAA Paper 77-1301, October 1977.

12. Wright, S. E.: Waveguides and Rotating Sources. J. of Sound and Vibration, vol. 25, no. 1, 1972, pp. 163-178.

13. Tester, B. J.: The Propagation and Attenuation of Sound in Lined Ducts Containing Uniform or "Plug" Flow. J. of Sound and Vibration, vol. 28, no. 2, 1973, pp. 151-203.

14. Lester, H. C.; and Posey, J. W.: Optimal One-Section Circular Sound-Absorbing Duct Liners for Plane-Wave and Monopole Sources Without Flow. NASA TN D-8348, December 1976.

15. Felsen, L. B.; and Yee, H. Y.: Ray Method for Sound-Wave Reflection in an Open-Ended Circular Pipe. J. Acoust. Soc. America, vol. 44, no. 4, October 1968, pp. 1028-1039.

16. Kornhauser, E. T.: Ray Theory for Moving Fluids. J. Acoust. Soc. America, vol. 25, no. 5, September 1953, pp. 945-949.

17. Doak, P. E.: The Reflection of a Spherical Acoustic Pulse by an Absorbent Infinite Plane and Related Problems. Proceedings of the Royal Society (London), vol. A 215, 1952, pp. 233-254.

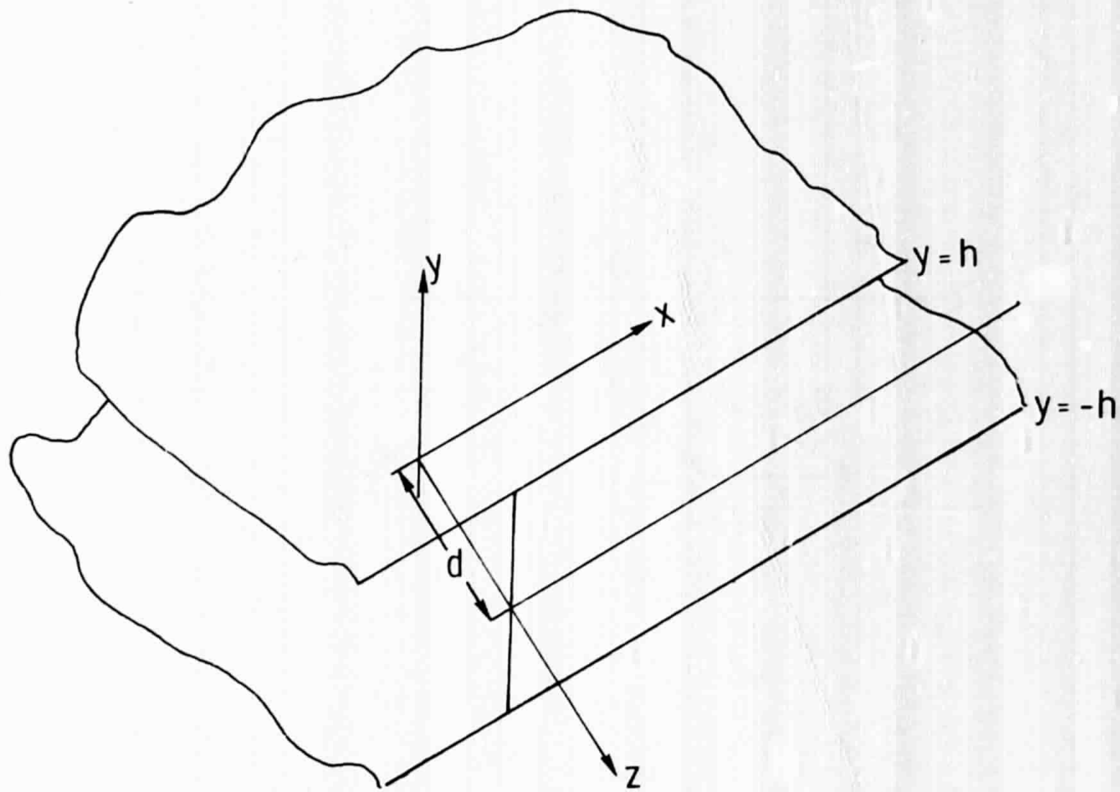

Figure 1.- Parallel plate duct coordinate system.

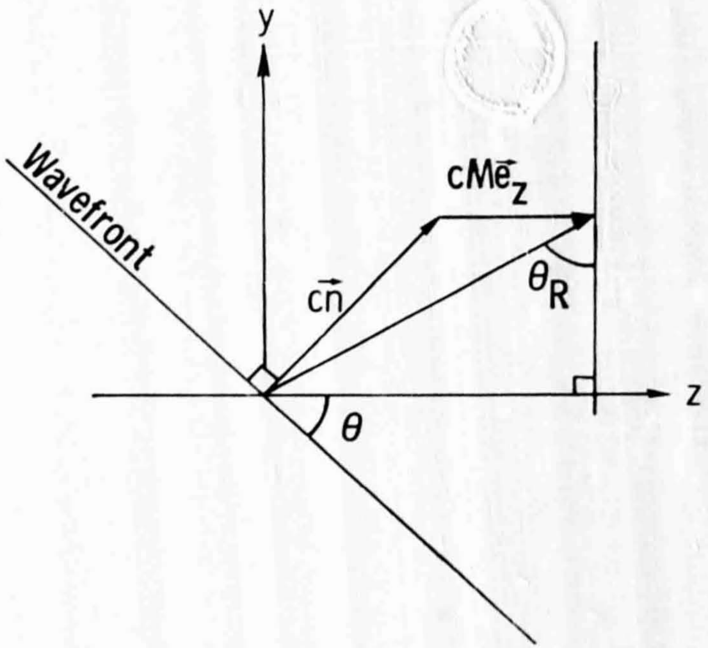

Figure 2.- Vector relationship between the unit wavefront normal $\vec{n}$ and the associated ray direction for a plane wave in a homogeneous medium moving with uniform flow velocity $cM\vec{e}_z$.

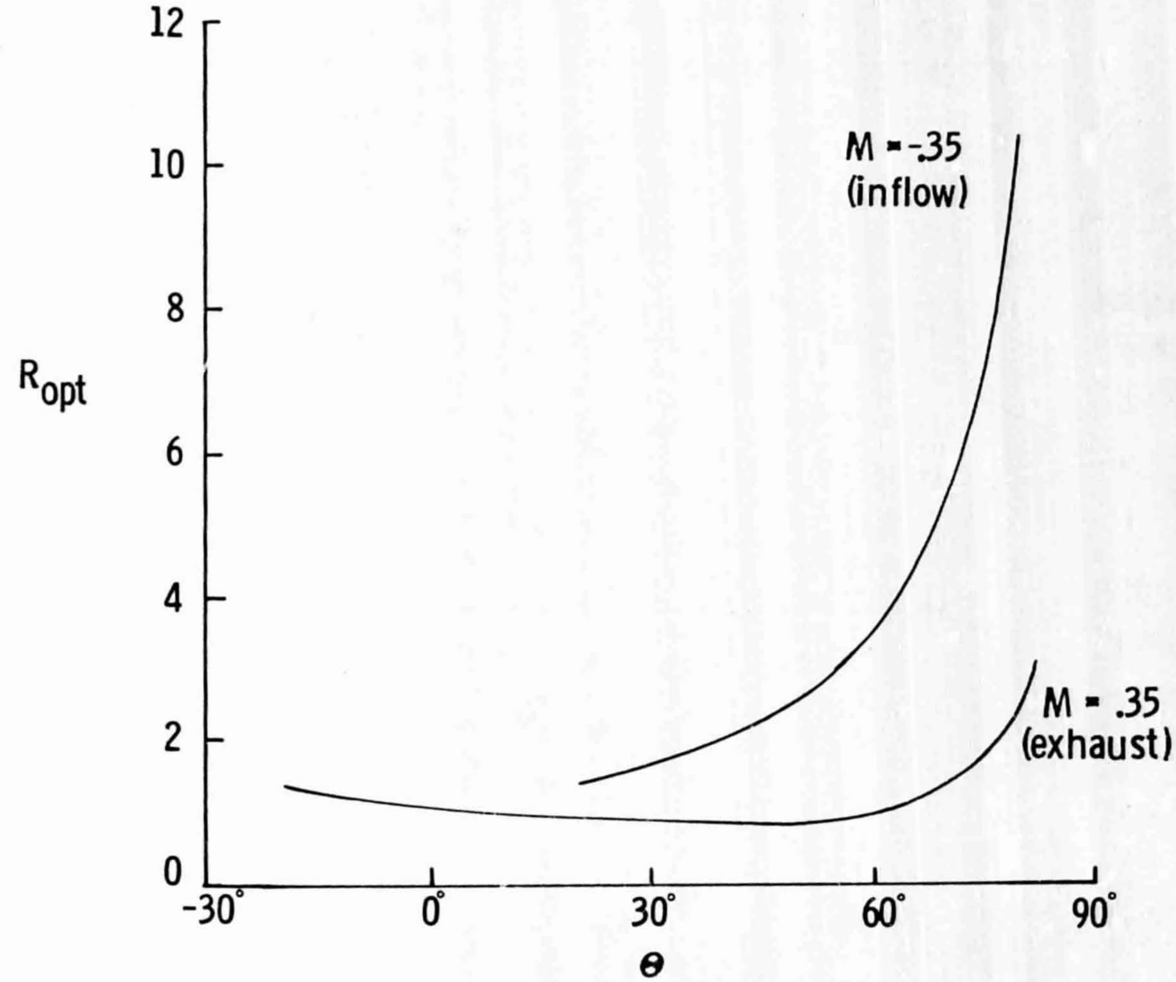

Figure 3.- Optimal parallel plate duct liner resistance R_{opt} as a function of wavefront orientation angle θ for sample inflow and exhaust conditions.

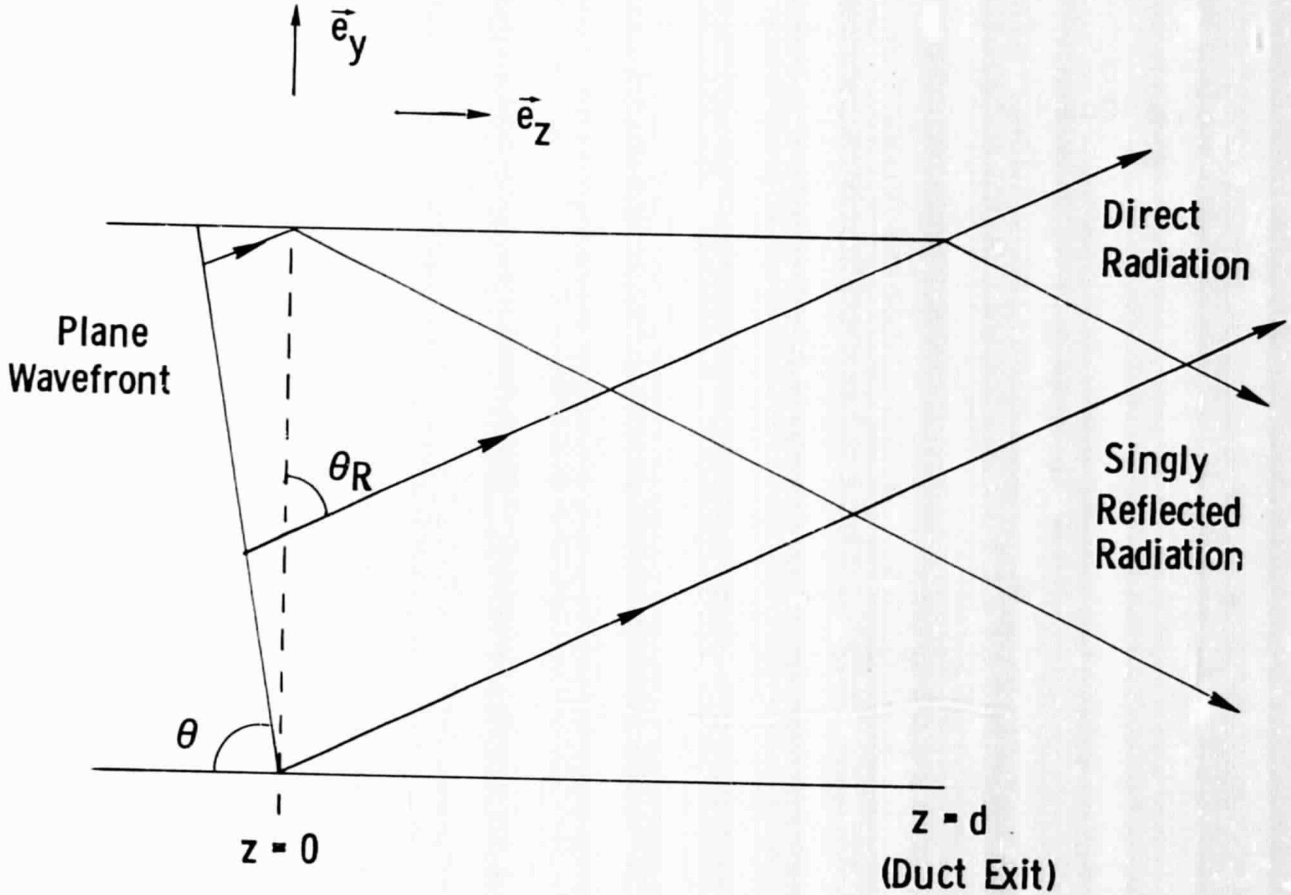

Figure 4.- Schematic showing direct and singly reflected radiation from duct termination due to a non-axial plane wave at $z = 0$.

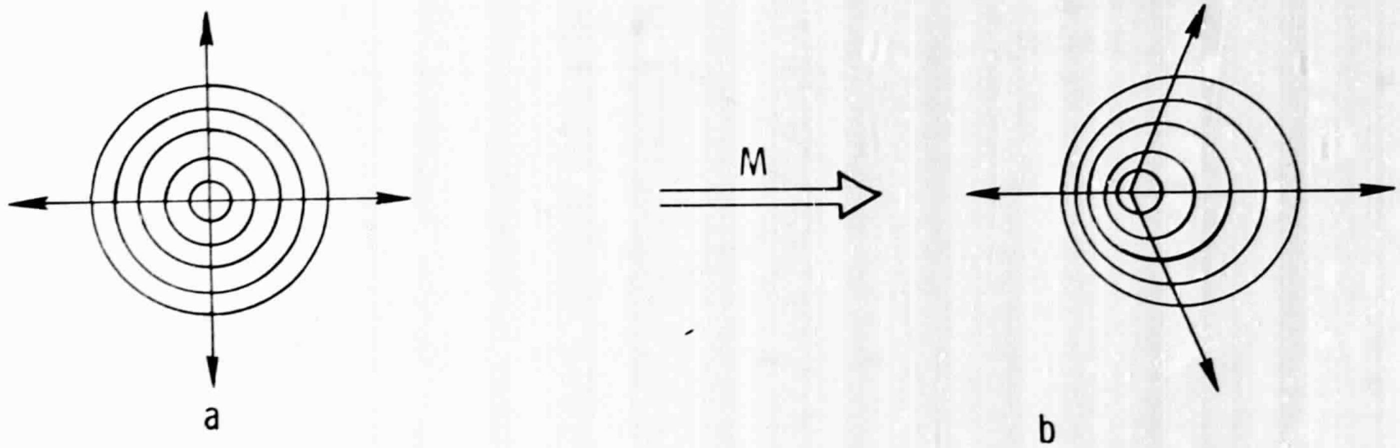

Figure 5.- Schematics of spherical wavefront spreading associated with a point source: a) medium at rest, b) medium in uniform subsonic motion.

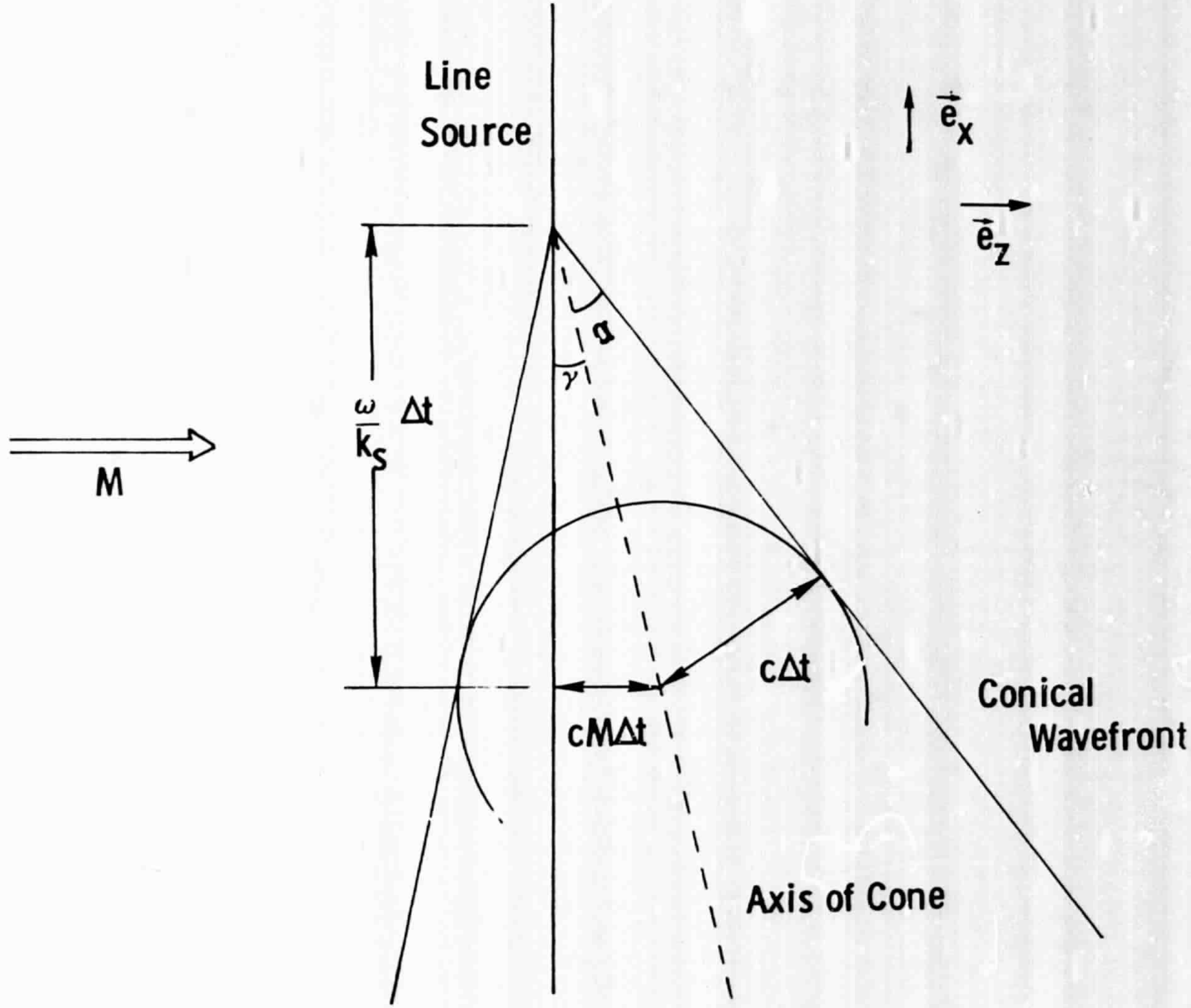

Figure 6.- Geometry of a conical wavefront due to a stationary line source having spatial variation $e^{ik_s x}$ and time dependence $e^{-i\omega t}$ in a homogeneous medium with uniform flow velocity $cM\vec{e}_z$. The crossection of the cone shown is in the plane defined by the line source and the flow velocity vector.

1. Report No. NASA TM 78708	2. Government Accession No.	3. Recipient's Catalog No.
4. Title and Subtitle High Frequency Sound Attenuation in Short Flow Ducts		5. Report Date May 1978
		6. Performing Organization Code 2640
7. Author(s) J. W. Posey		8. Performing Organization Report No.
9. Performing Organization Name and Address NASA Langley Research Center Hampton, Virginia 23665		10. Work Unit No. 505-03-13-12
		11. Contract or Grant No.
12. Sponsoring Agency Name and Address National Aeronautics and Space Administration Washington, DC 20546		13. Type of Report and Period Covered Technical Memorandum
		14. Sponsoring Agency Code

15. Supplementary Notes

Paper to be presented at the 95th Meeting of the Acoustical Society of America, Providence, Rhode Island, May 16-19, 1978.

16. Abstract

A geometrical acoustics approach is proposed as a practical design tool for absorbent liners in such short flow ducts as may be found in turbofan engine nacelles. As an example, a detailed methodology is presented for three different types of sources in a parallel plate duct containing uniform ambient flow. A plane wave whose wavefronts are not normal to the duct walls, an arbitrarily located point source, and a spatially harmonic line source are each considered. Optimal wall admittance distributions are found, and it is shown how to estimate the insertion loss for any admittance distribution. It is suggested that the extension of the methodology to realistic source distributions in variable area cylindrical or annular ducts containing arbitrary flow is conceptually straightforward and computationally practical on a vector-hardware digital computer.

17. Key Words (Suggested by Author(s)) Duct acoustics Acoustical liners Sound Attenuation Geometrical Acoustics 71		18. Distribution Statement Unclassified Unlimited	
19. Security Classif. (of this report) Unclassified	20. Security Classif. (of this page) Unclassified	21. No. of Pages 23	22. Price* $4.00

* For sale by the National Technical Information Service, Springfield, Virginia 22161